



# Applications of Machine Learning in Molecular Dynamics

*Yuan Hu*

*Shichun Wang*

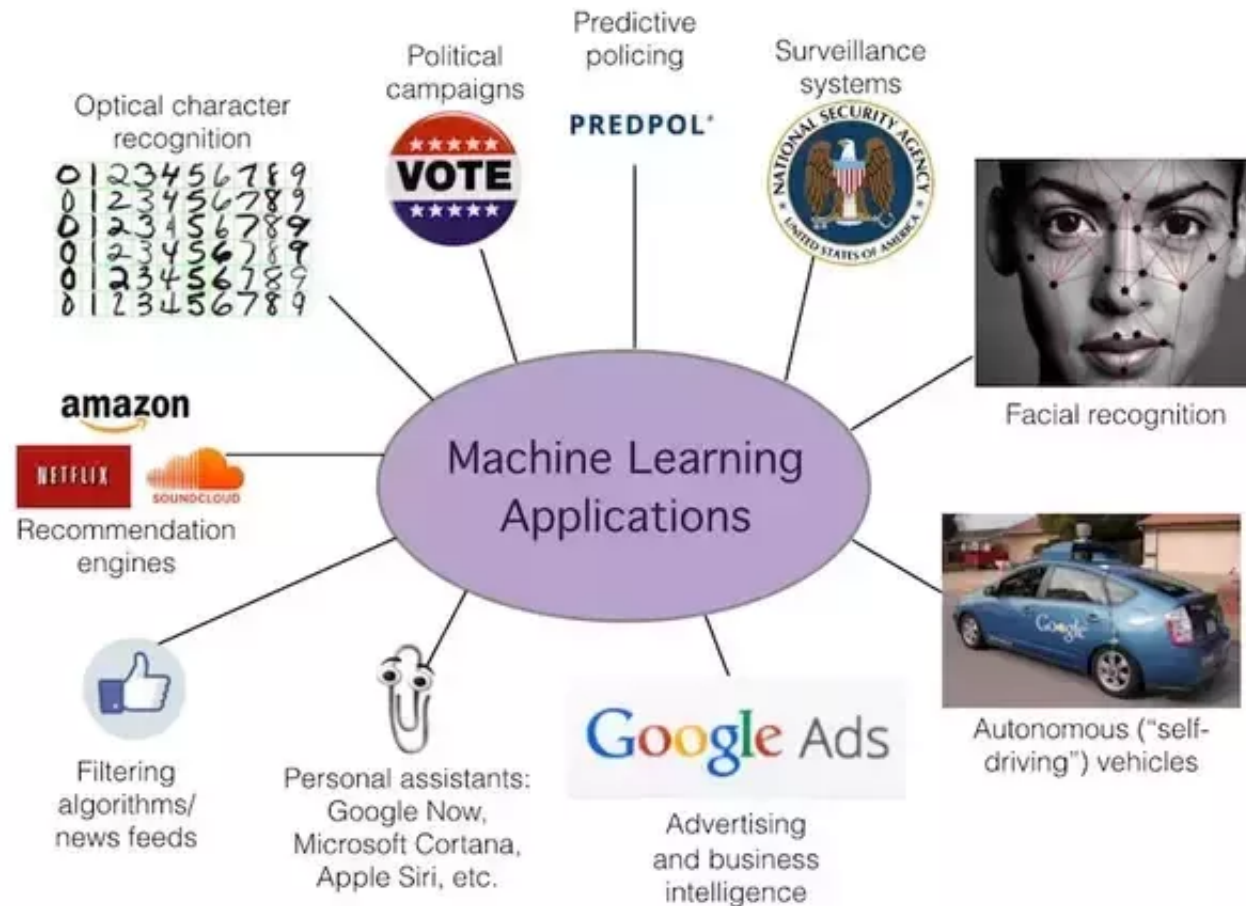
*Size Zheng*

**USC**

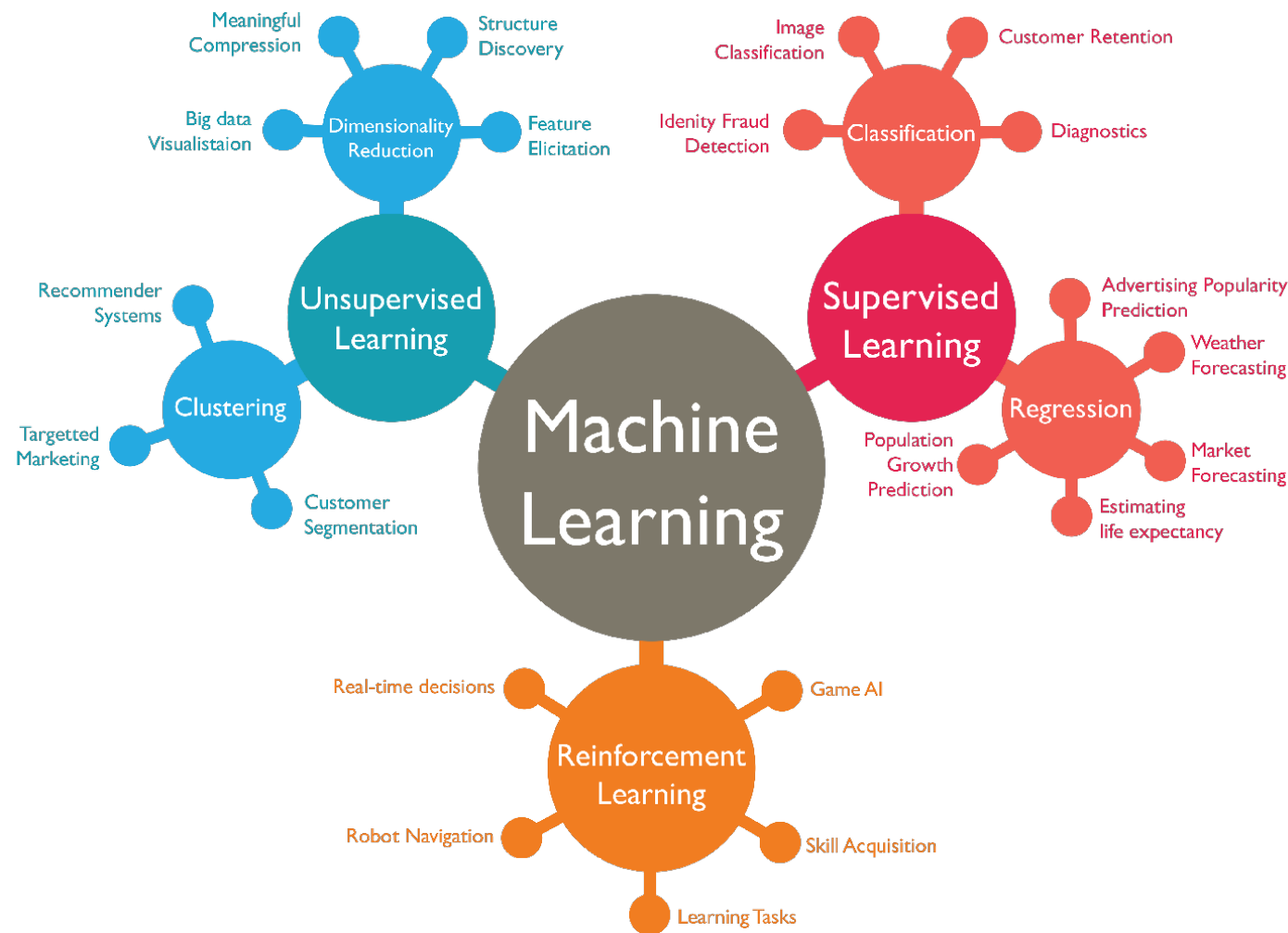
School of Engineering

Mork Family Department of Chemical Engineering & Materials Science

University of Southern California



[https://redshiftzero.github.io/assets/manip/ml\\_applications.png](https://redshiftzero.github.io/assets/manip/ml_applications.png)



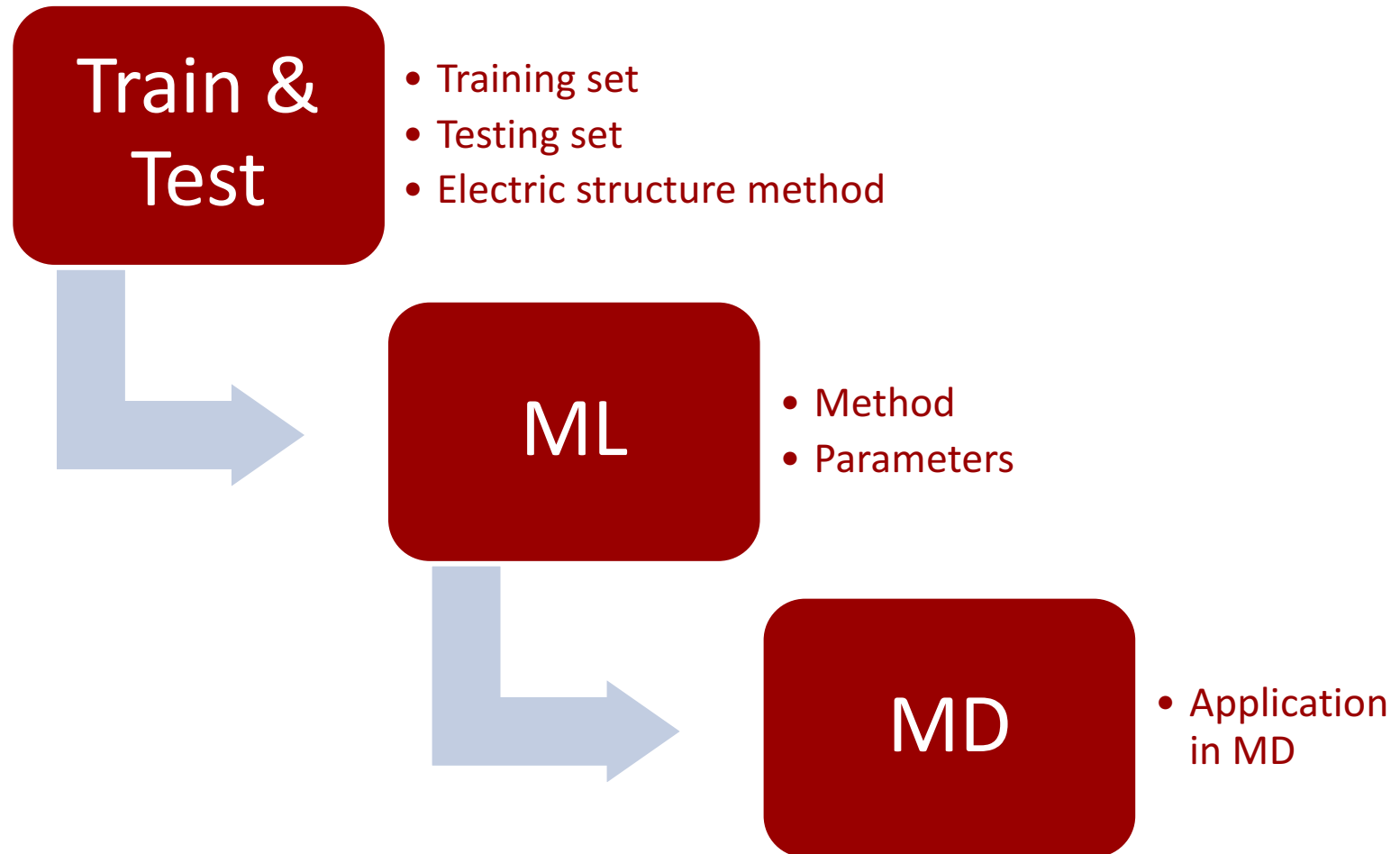


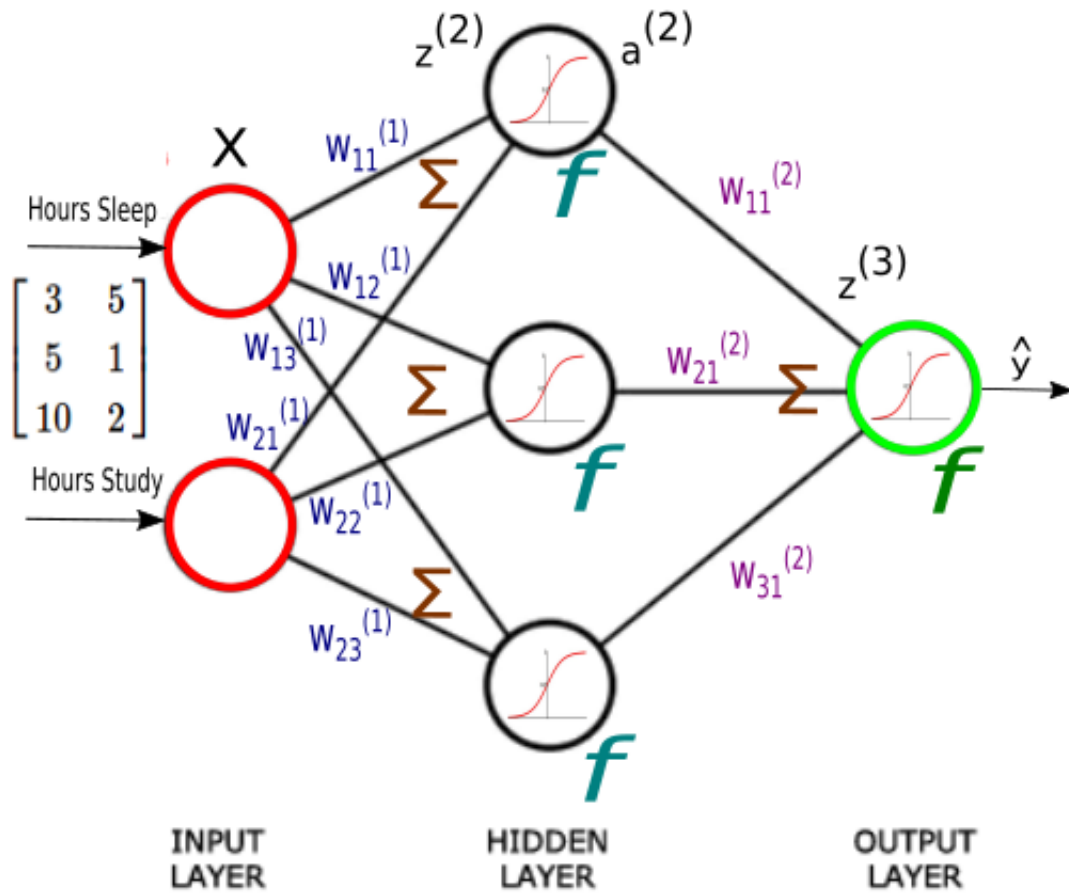
In *ab initio* MD, the energies and forces need to be calculated “on-the-fly”: very expensive

- Energies can be fitted to high accuracy with very small remaining errors compared to the underlying reference data
- Energies can be calculated efficiently and require much less CPU time than electronic structure calculations.
- No knowledge about the functional form of the PES is required.
- The energy expression is unbiased, generally applicable to all types of bonding and does not require system-specific modification



- Neural Network Potential (NNP)
- Kernel Ridge Regression (KRR)
- Gaussian Approximation Potential (GAP)





Forwarding

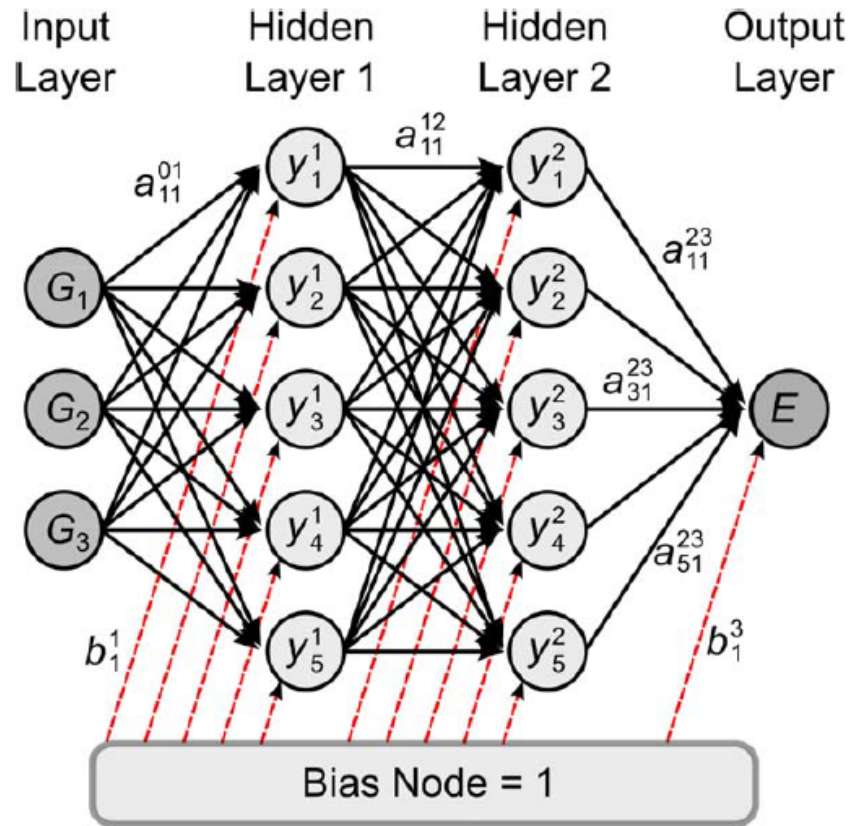
$$O = \text{activation function}(W \cdot I)$$

Backpropagating

$$\frac{\partial E}{\partial w_{jk}} = -2(t_k - o_k) \cdot$$

$$\frac{\partial}{\partial w_{jk}} \text{activation function}(\sum_j w_{jk} \cdot o_j)$$

$$\text{new } w_{jk} = \text{old } w_{jk} - \alpha \frac{\partial E}{\partial w_{jk}}$$

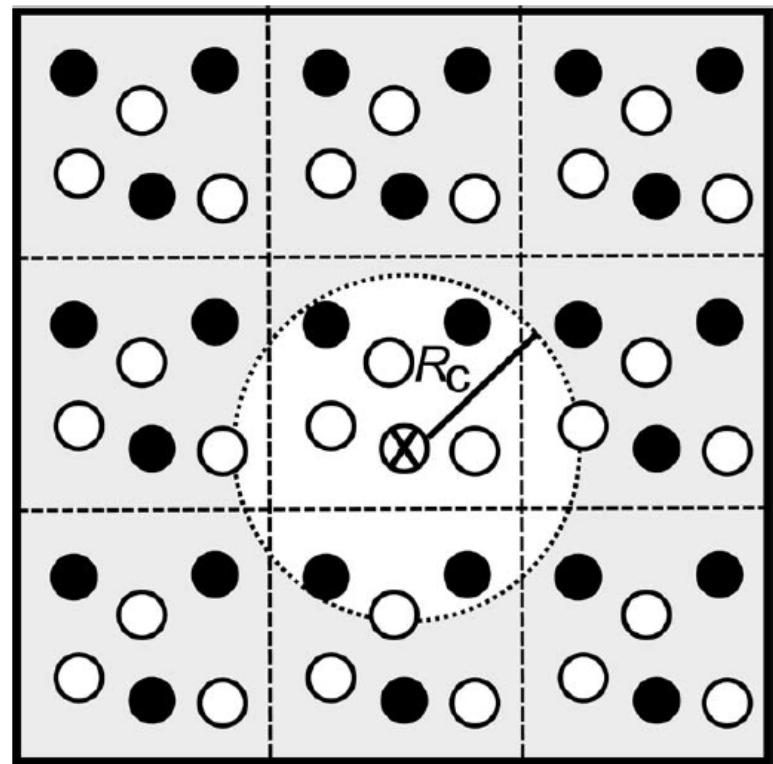
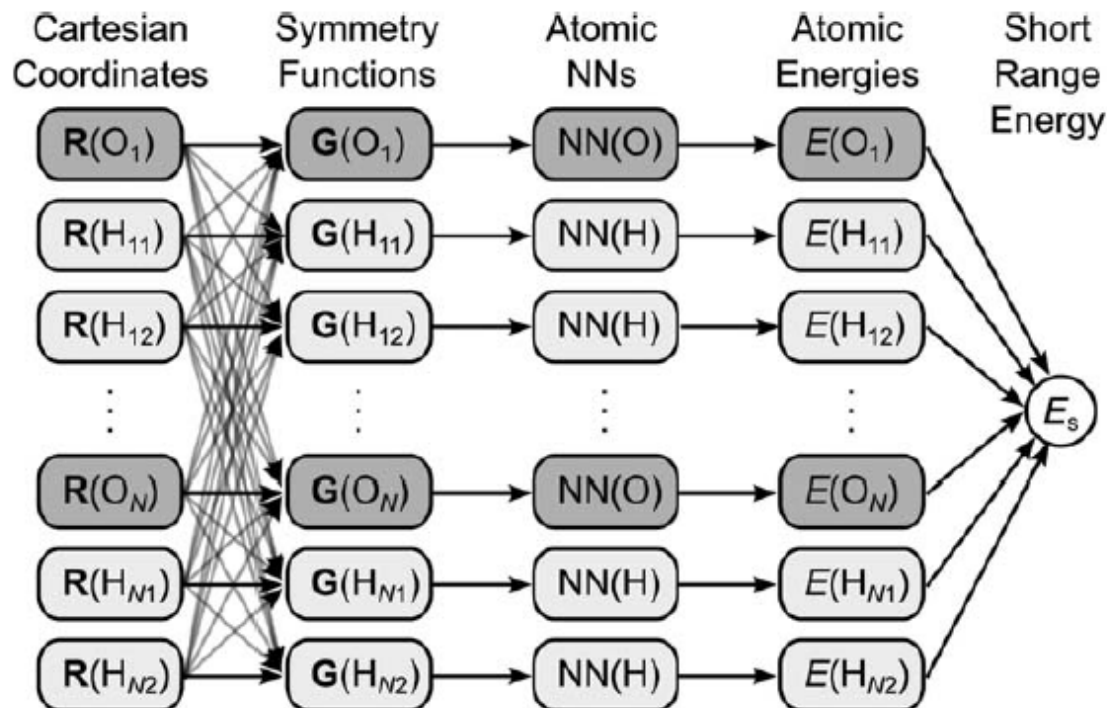


$$y_i^j = f_i^j \left( b_i^j + \sum_{k=1}^{N_{j-1}} a_{k,i}^{j-1,j} \cdot y_k^{j-1} \right)$$



For High-dimensional NNPs, using a single NN for the construction of high dimensional NNPs is impossible.

- Too many input nodes make the construction of the NNP inefficient
- Symmetry of the NN
- Not scalable



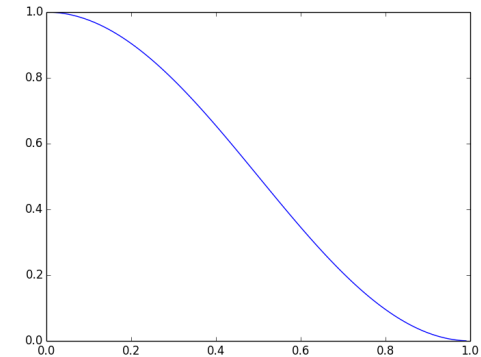
$$E = E_s + E_{\text{elec}} = \sum_{i=1}^{N_{\text{atom}}} E_i + E_{\text{elec.}}$$



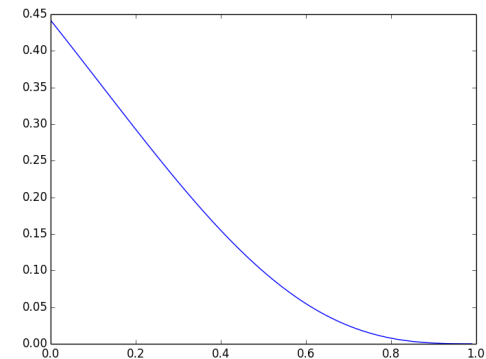
# Symmetry Function

The cut-off function  $f_c$

$$f_{c,1}(R_{ij}) = \begin{cases} 0.5 \cdot \left[ \cos\left(\frac{\pi R_{ij}}{R_c}\right) + 1 \right] & \text{for } R_{ij} \leq R_c \\ 0.0 & \text{for } R_{ij} > R_c \end{cases}$$



$$f_{c,2}(R_{ij}) = \begin{cases} \tanh^3 \left[ 1 - \frac{R_{ij}}{R_c} \right] & \text{for } R_{ij} \leq R_c \\ 0.0 & \text{for } R_{ij} > R_c \end{cases}$$





# Symmetry Function

$$G_i^1 = \sum_{j=1}^{N_{\text{atom}}} f_c(R_{ij})$$

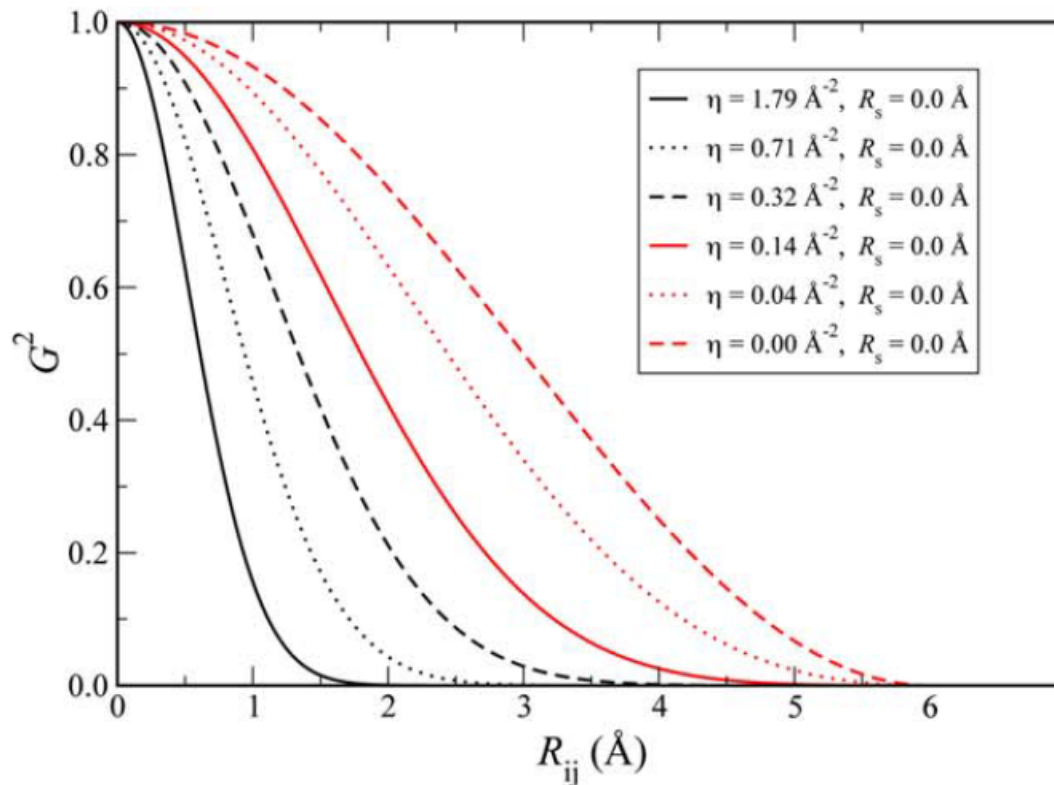
$$G_i^2 = \sum_{j=1}^{N_{\text{atom}}} e^{-\eta(R_{ij}-R_s)^2} \cdot f_c(R_{ij})$$

$$G_i^3 = 2^{1-\zeta} \sum_{j \neq i} \sum_{k \neq i,j} \left[ (1 + \lambda \cdot \cos \theta_{ijk})^\zeta \cdot e^{-\eta(R_{ij}^2 + R_{ik}^2 + R_{jk}^2)} \cdot f_c(R_{ij}) \cdot f_c(R_{ik}) \cdot f_c(R_{jk}) \right]$$

$$G_i^4 = 2^{1-\zeta} \sum_{j \neq i} \sum_{k \neq i,j} \left[ (1 + \lambda \cdot \cos \theta_{ijk})^\zeta \cdot e^{-\eta(R_{ij}^2 + R_{ik}^2)} \cdot f_c(R_{ij}) \cdot f_c(R_{ik}) \right]$$



# Symmetry Function - Example



$$G_i^2 = \sum_{j=1}^{N_{\text{atom}}} e^{-\eta(R_{ij}-R_s)^2} \cdot f_c(R_{ij})$$

Jorg Behler, *International Journal of Quantum Chemistry* 2015, 115, 1032–1050

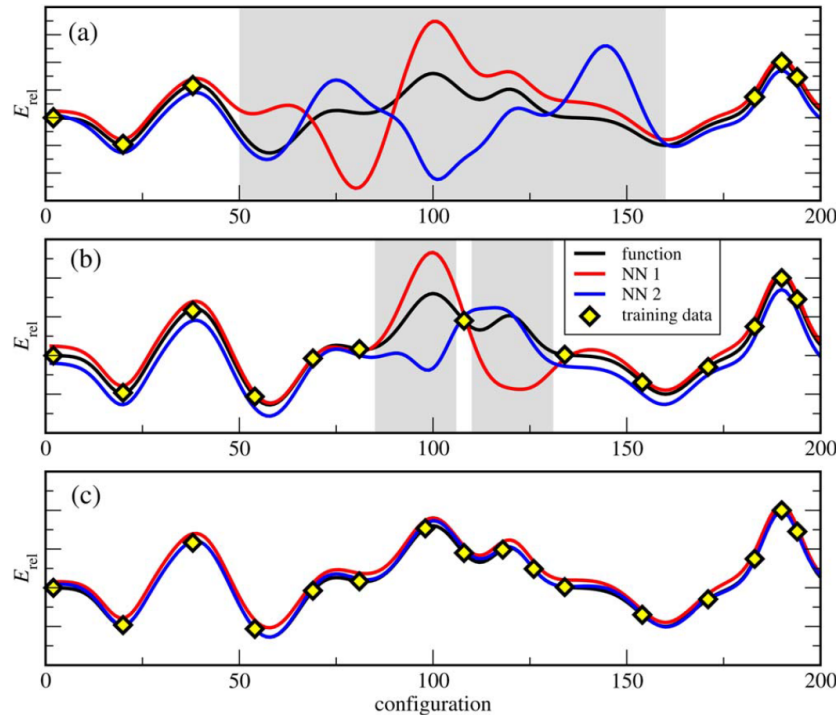
USC

School of Engineering

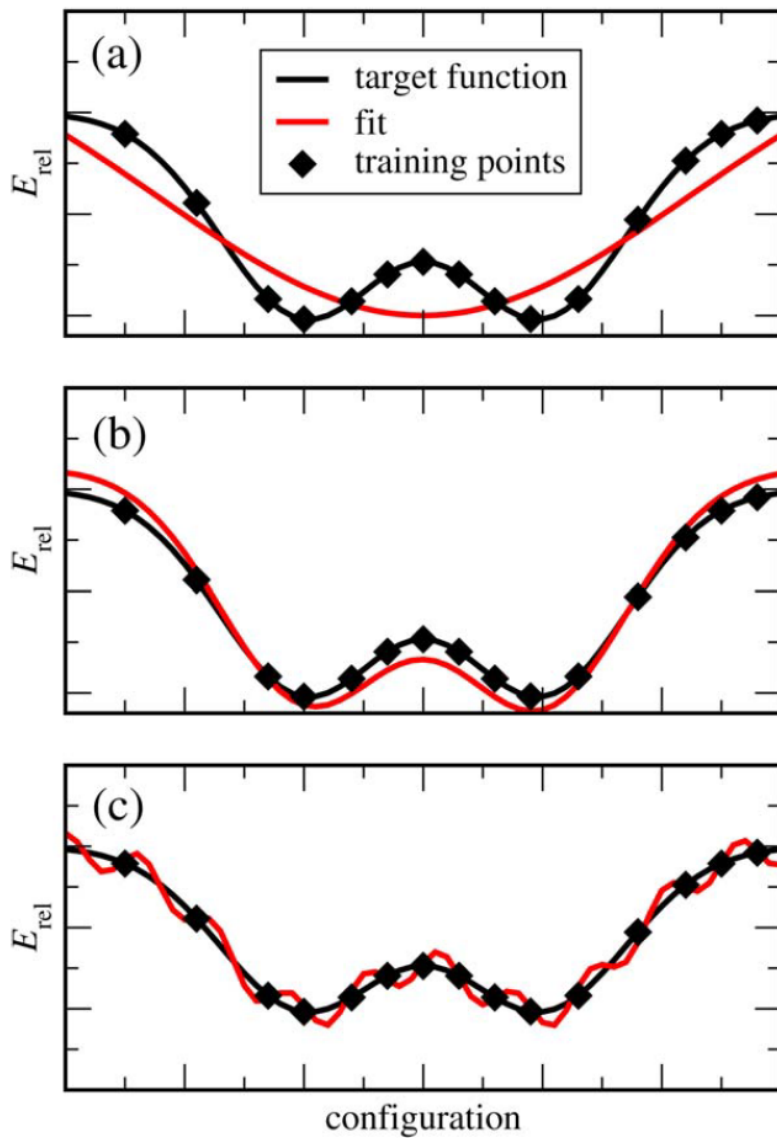
University of Southern California



# Training NNs



1. Select an electronic structure method.
2. Define a first set of structures and determine the energies and forces.
3. Construct a first preliminary NNP
4. Carry out simulations using this NNP to find structures, give rise to extrapolation warnings or unphysical geometries.
5. Determine the electronic structure energies and forces of these structures, include them in the training set and improve the NNP.
6. Improve the NNP systematically and self-consistently by running NNP-based simulations using the multiple>NNP method.
7. As soon as no further warnings, the NNP is ready to use.



### Weight Parameters

- Random numbers
- Different optimization algorithms to improve them

### The architecture of the NNs

- Empirical
- Identify a suitable number of hidden layers and nodes per layer is simply to carry out a number of fits and to select the one with the lowest errors of the energies and forces in the test set.

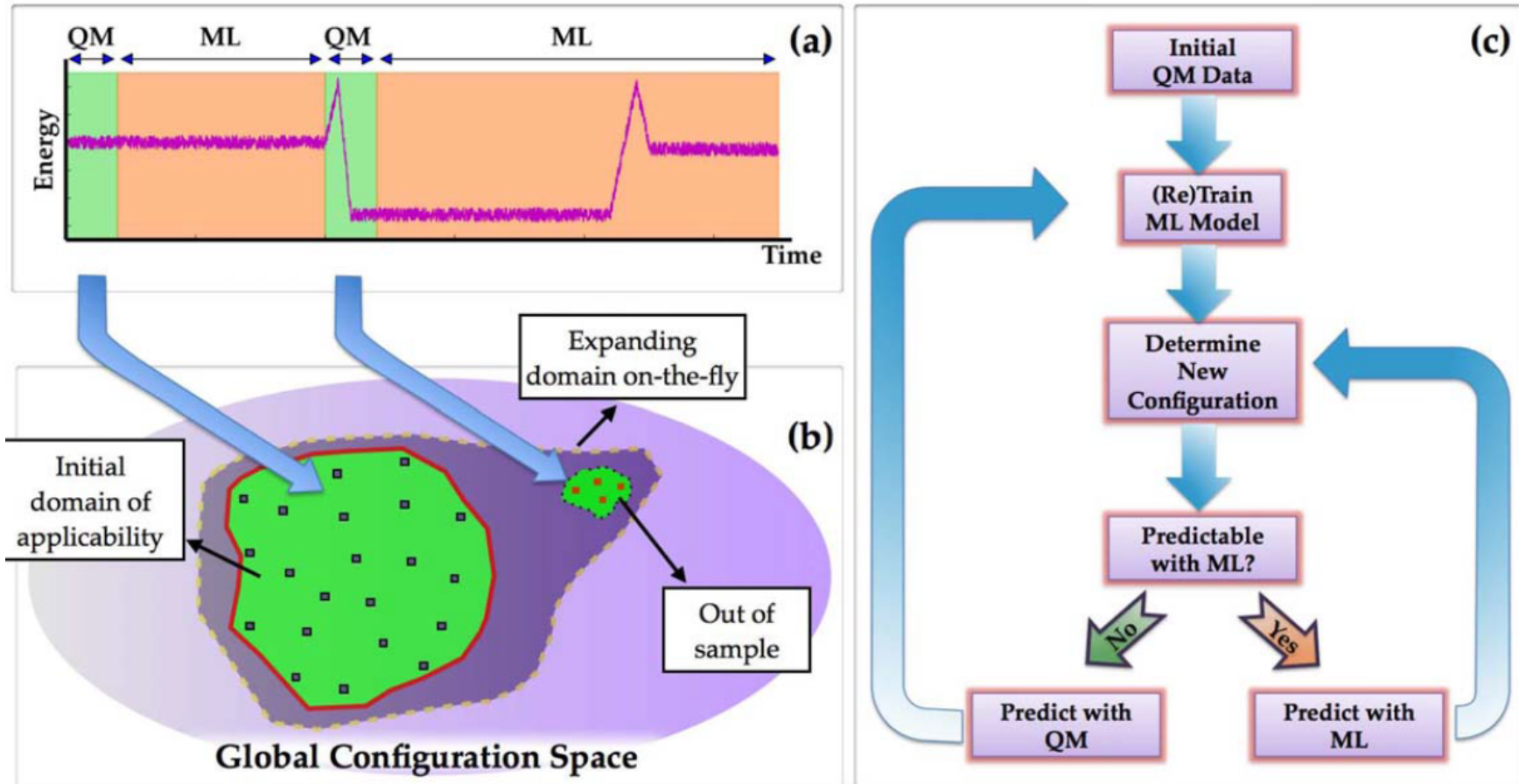


## Disadvantages:

- The evaluation of NNPs is notably slower than the use of simple classical force fields.
- NNPs have no physical basis and only very limited extrapolation capabilities.
- The construction of NNPs requires substantial effort, and a large number of training points from electronic structure calculations is required.
- Currently, NNPs are limited to systems containing either only a few different chemical elements but many atoms or a small number of atoms with arbitrary nuclear charges.



# Adaptive Machine Learning Framework



The significant redundancies implicit in conventional ab initio MD schemes can be systematically eliminated.

V. Botu, R. Ramprasad, *International Journal of Quantum Chemistry* 2015, 115, 1074–1083



- To simulate 32 atom bulk Al, to use ML method, each prediction takes roughly a millisecond.
- For comparison, the same case with DFT will take about 45 min on a 16 core machine, a speed up on the order of  $10^6$ !

USC

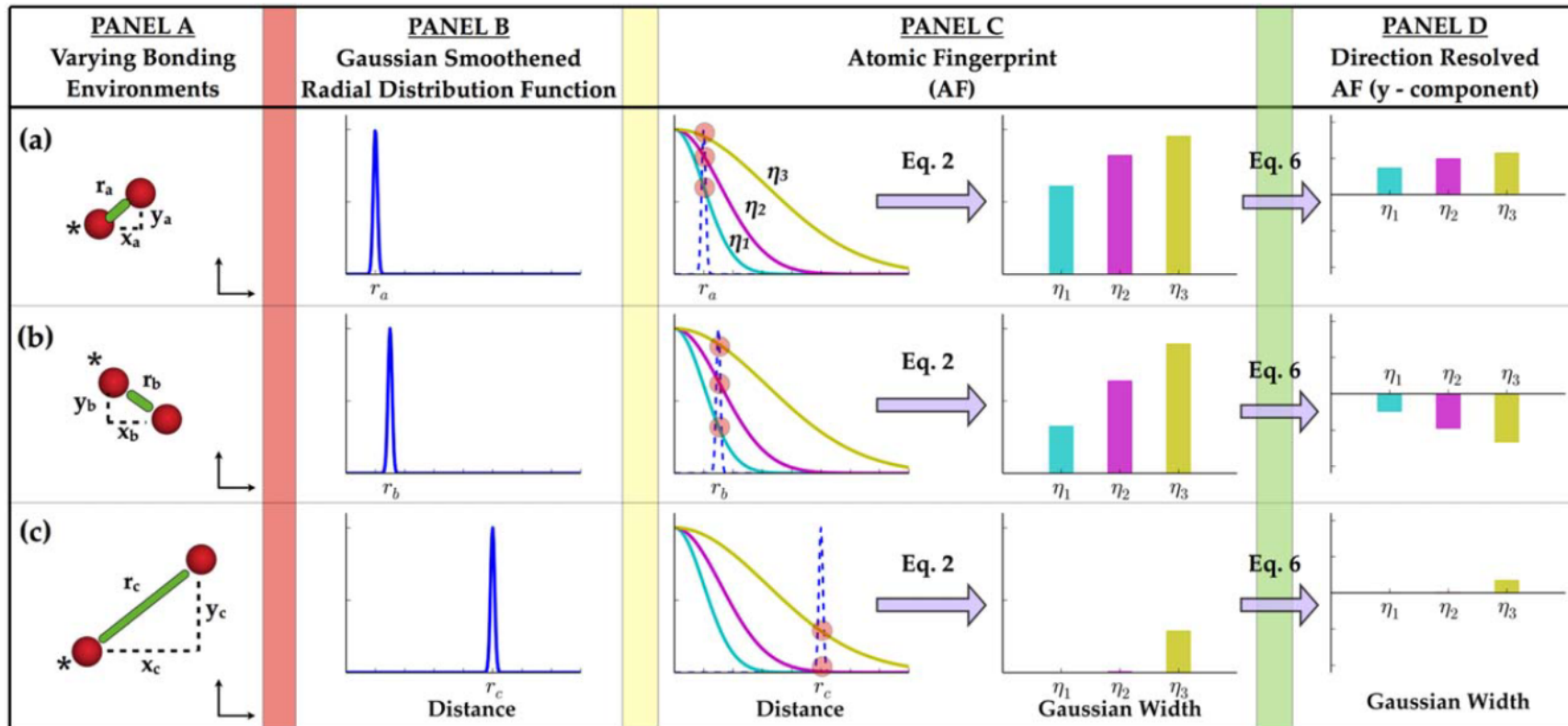
School of Engineering

V. Botu, R. Ramprasad, *International Journal of Quantum Chemistry* 2015, 115, 1074–1083

University of Southern California



# Symmetry Function



$$V_i^k(\eta) = \sum_{j \neq i} \left[ \frac{r_{ij}^k}{r_{ij}} e^{-\eta(R_{ij}-R_s)^2} \cdot f_c(R_{ij}) \right], k \in \{x, y, z\}$$

V. Botu, R. Ramprasad, *International Journal of Quantum Chemistry* 2015, 115, 1074–1083

USC

School of Engineering

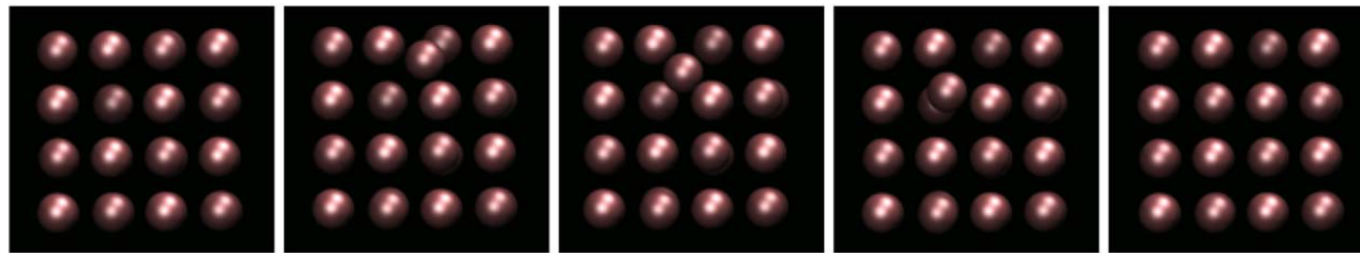
University of Southern California



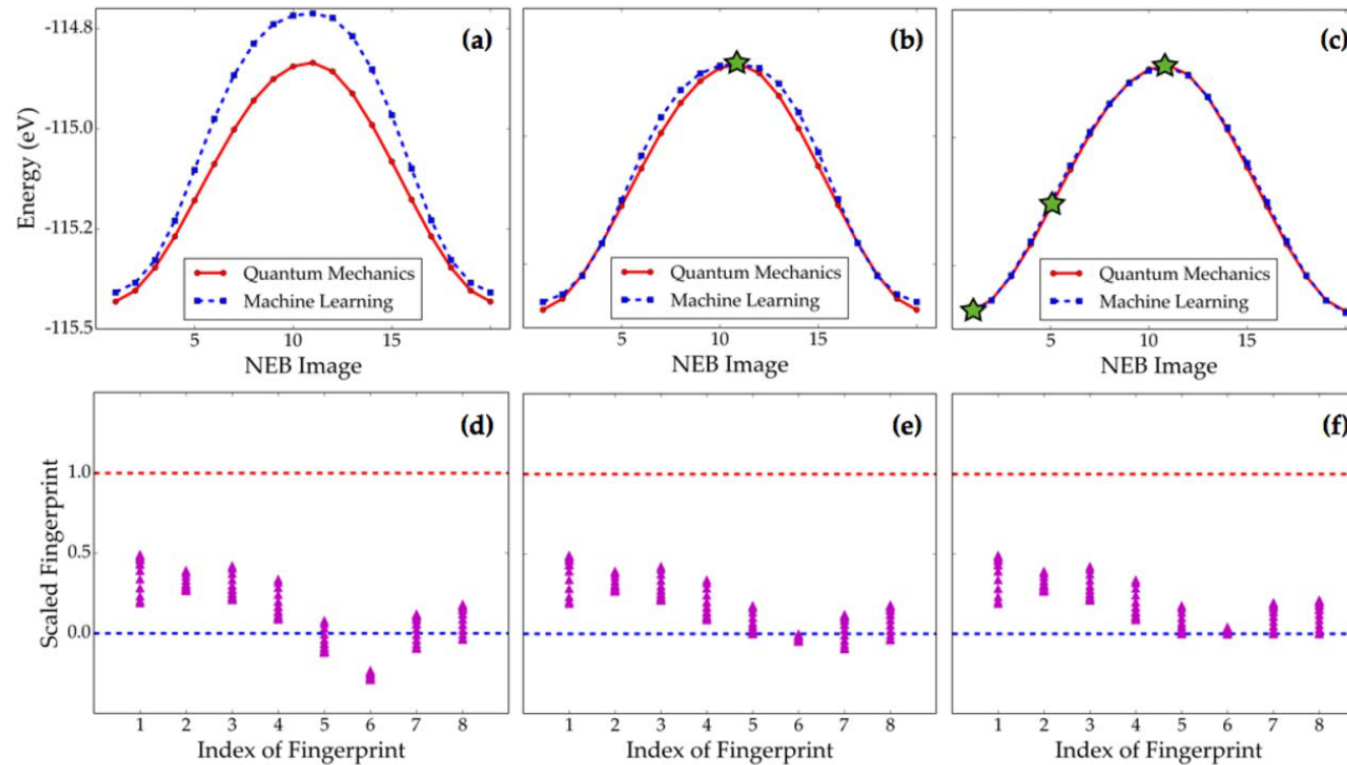
## Machine Learning Method – Kernel Ridge Regression

KRR transforms the input fingerprint into a higher dimensional space whereby a linear relation between the transformed fingerprint and the property of interest can be established. To be precise, the mapping process between the fingerprint and property involves the “distances” between fingerprints rather than the fingerprints themselves. KRR may thus be viewed as a similarity-based learning method, that is, similar fingerprints will lead to similar properties.

$$P_u = \sum_v \alpha_v e^{-\frac{1}{2} \left( \frac{|d_{uv}|}{\sigma} \right)^2}$$



Vacancy migration within bulk Al correspond to steps 1, 5, 10, 15, and 20.



a) and d) with no retraining, b) and e) with the TS added to training and c) and f ) with TS and image 1 and 5 added to the training.

V. Botu, R. Ramprasad, *International Journal of Quantum Chemistry* 2015, 115, 1074–1083



# Introduction to Atomic Energy Network (aenet) Package

USC

School of Engineering

University of Southern California

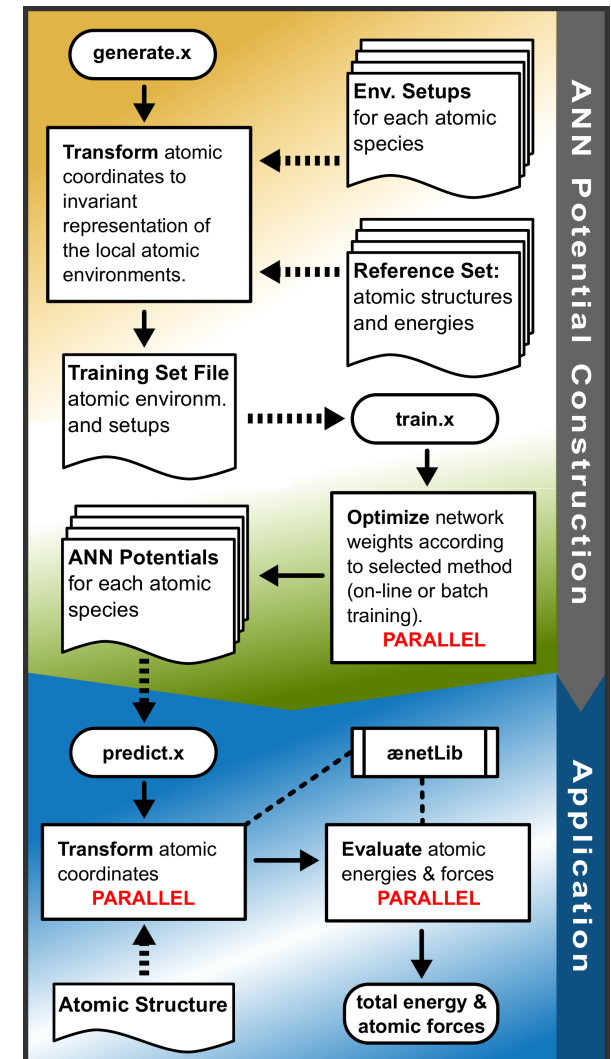
# Atomic Energy Network - aenet



- Open source <http://ann.atomistic.net>
- Potential construction tools
  - generate.x – preprocessing
  - train.x – train ANN force field
- Application tools
  - predict.x – get forces from atomic coordinates
  - aenetLib – interface to other program

## Train neural network force field

- Activation functions
  - linear function  $f_a^1(x) = x,$
  - hyperbolic tangent  $f_a^2(x) = \tanh(x) = \frac{1-e^{-2x}}{1+e^{-2x}},$
  - logistic function  $f_a^3(x) = \frac{1}{1+e^{-x}}, \text{ and}$
  - tanh with linear twisting  $f_a^4(x) = 1.7159 \tanh\left(\frac{2}{3}x\right) + ax,$
- Learning methods – batch and online
- Optimization methods – gradient descent, limited-memory BFGS, Levenberg-Marquardt



# Train an ANN Force Field ( $\text{TiO}_2$ ) via aenet



Generate reference data set

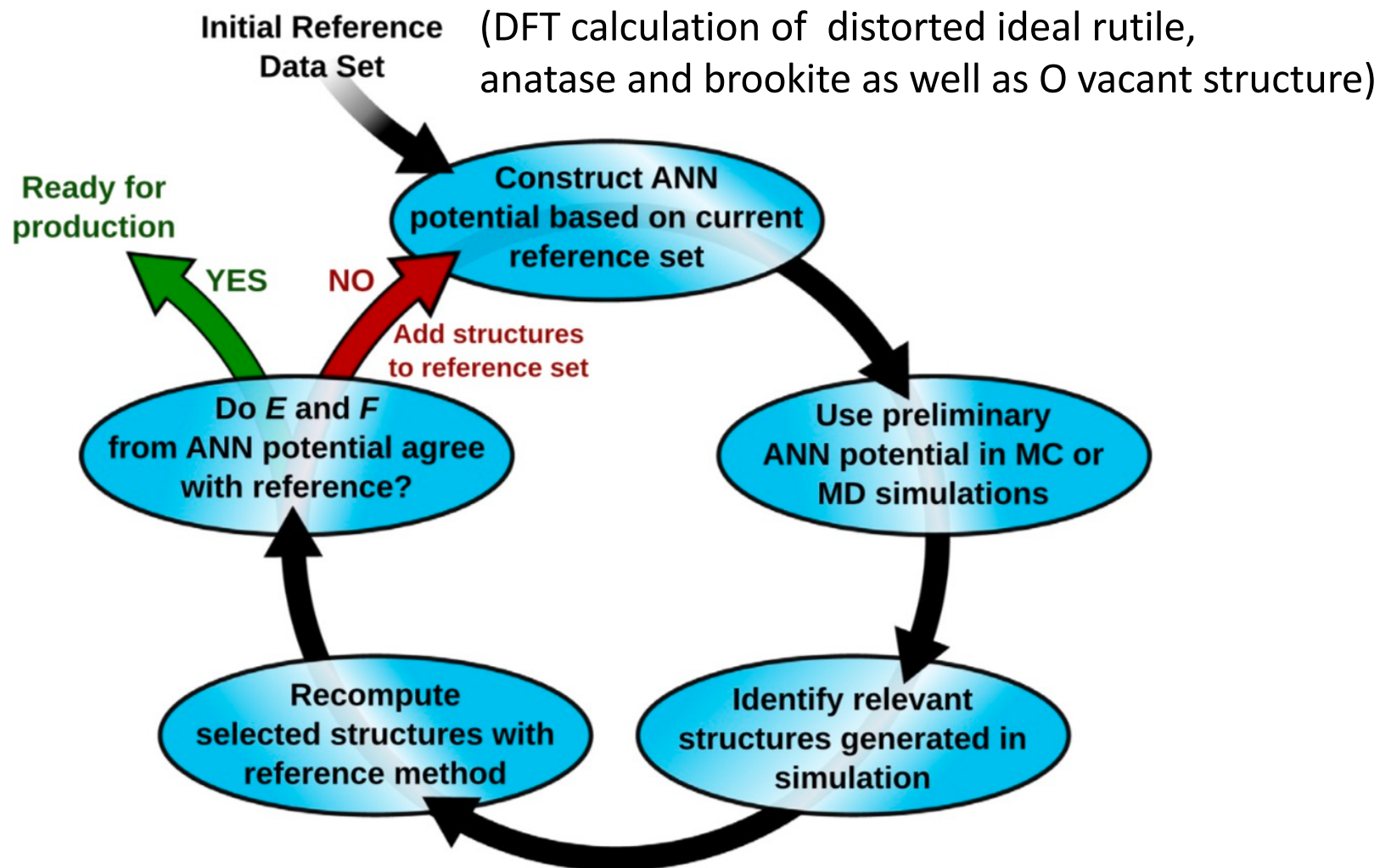
Set up structural fingerprint

Select network architecture

Select training method



# Generate reference data set



# Set up structural fingerprint



- 8 radial and 18 angular Behler-Parrinello basis functions for each combination of atomic species
- 8x2 (O, Ti) radial basis functions
- 18x3(O-O, Ti-Ti, O-Ti) angular basis functions
- Total 70 basis functions or nodes at the input layer

## Radial function – $\mathbf{G}^2$

$$G_i^2 = \sum_{j \neq i} e^{-\eta(R_{ij} - R_s)^2} \cdot f_c(R_{ij}), \quad f_c(R_{ij}) = \begin{cases} 0.5 \left[ \cos \left( \frac{\pi R_{ij}}{R_c} \right) + 1 \right] & \text{for } R_{ij} \leq R_c, \\ 0 & \text{for } R_{ij} > R_c. \end{cases}$$

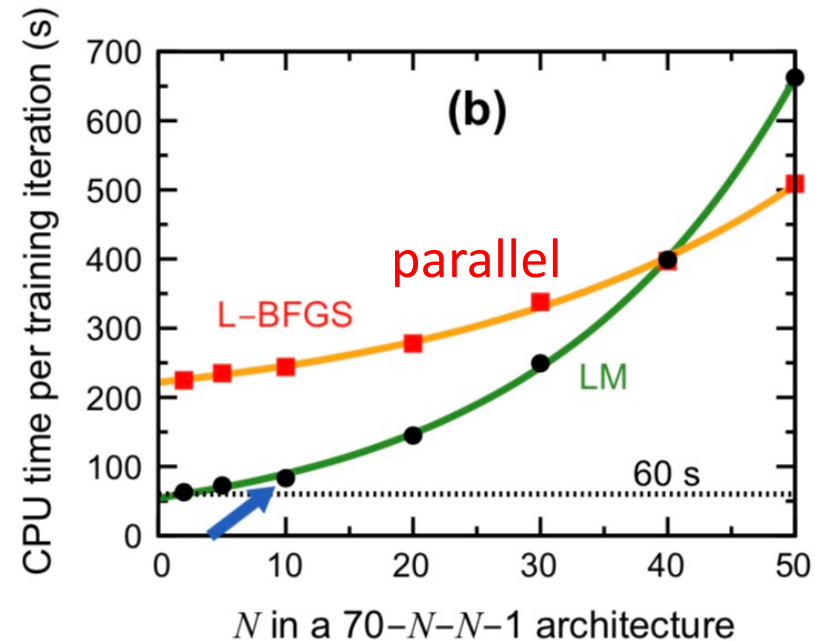
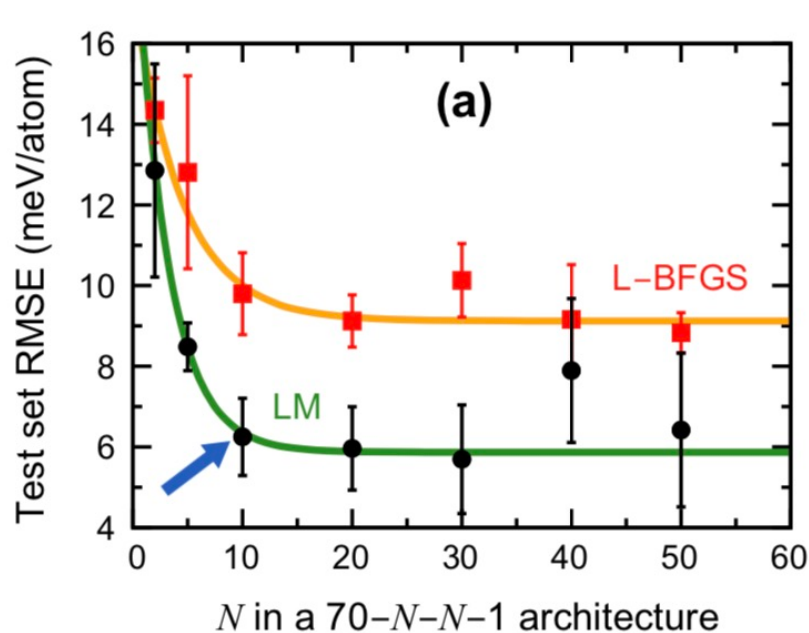
## Angular function – $\mathbf{G}^4$

$$G_i^4 = 2^{1-\zeta} \sum_{j \neq i} \sum_{k \neq i,j} (1 + \lambda \cos \theta_{ijk})^\zeta \cdot e^{-\eta(R_{ij}^2 + R_{ik}^2 + R_{jk}^2)} \cdot f_c(R_{ij}) \cdot f_c(R_{ik}) \cdot f_c(R_{jk}),$$

# Select the best network architecture



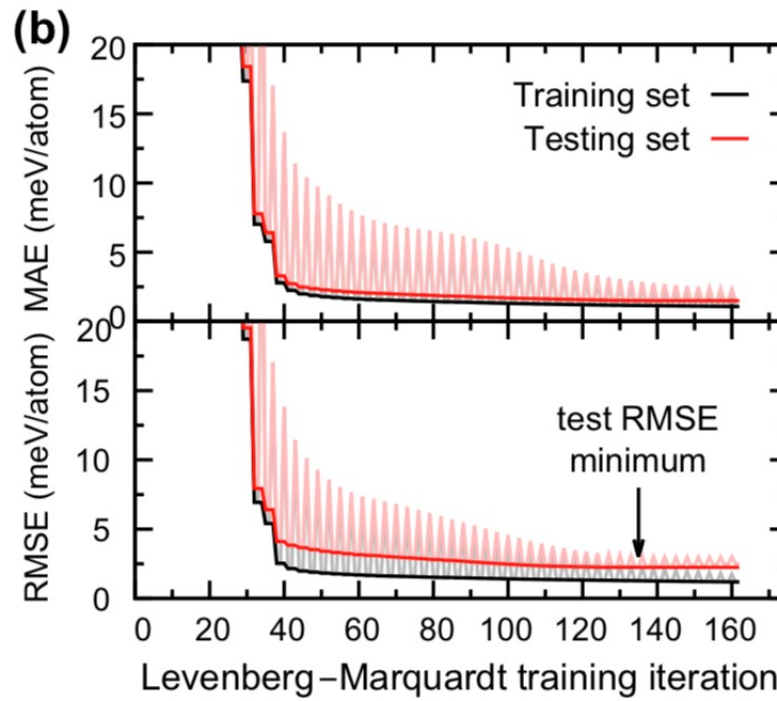
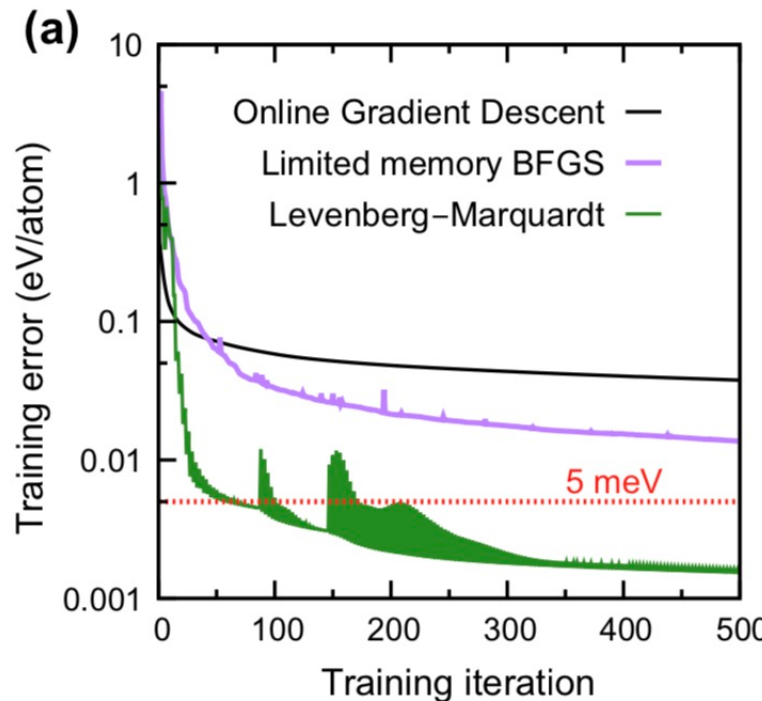
- The balance between model complexity and transferability (predictive power)
- Network architecture: # of network layers + # of nodes per network layer
- Too simple → poor transferability
- Too complex → poor efficiency and possible overfitting (poor transferability)





# Select training/optimization method

- 3 available training methods: online GD, LBGFS, Levenberg-Marquardt (LM)
- Online GD – least computationally demanding; any ANN architectures;  
**not well parallelized**
- Batch LBGFS – well parallelized; scales linearly with reference structures
- Batch LM – 2nd order convergence rate; needs to invert Hessian



# Evaluate the Trained ANN Force Field ( $\text{TiO}_2$ )

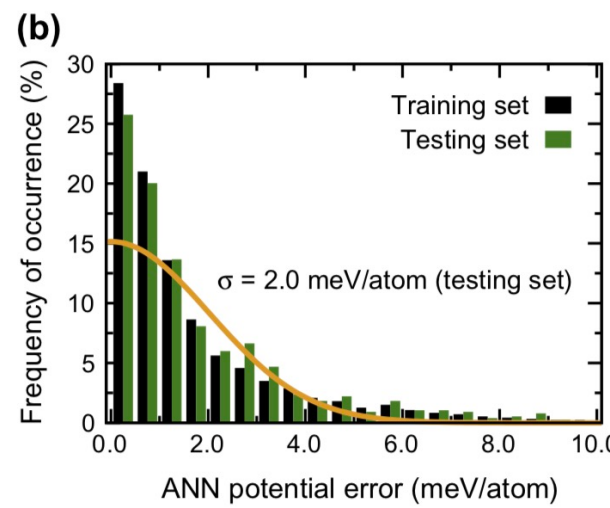
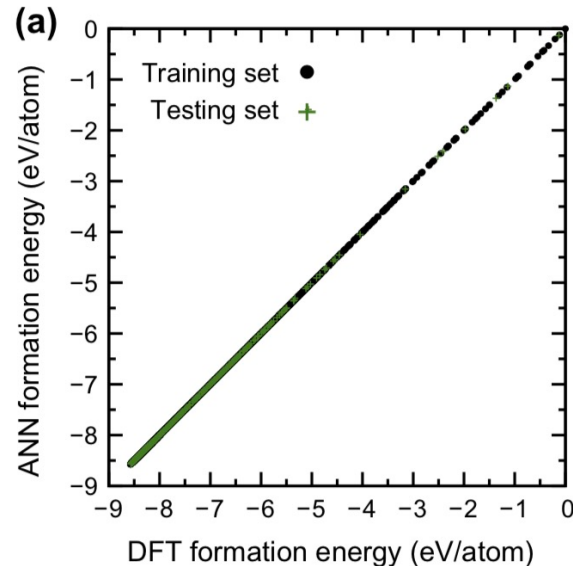


Accuracy of the ANN Potential

Reliability for MD simulations

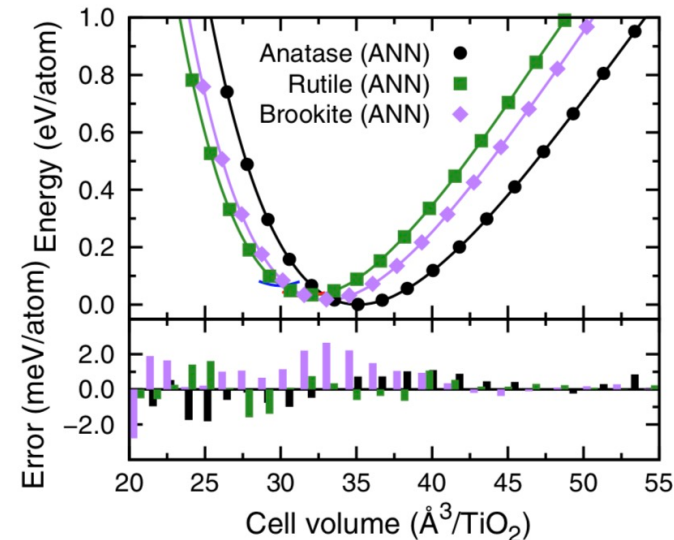


# Accuracy of the $\text{TiO}_2$ ANN Potential

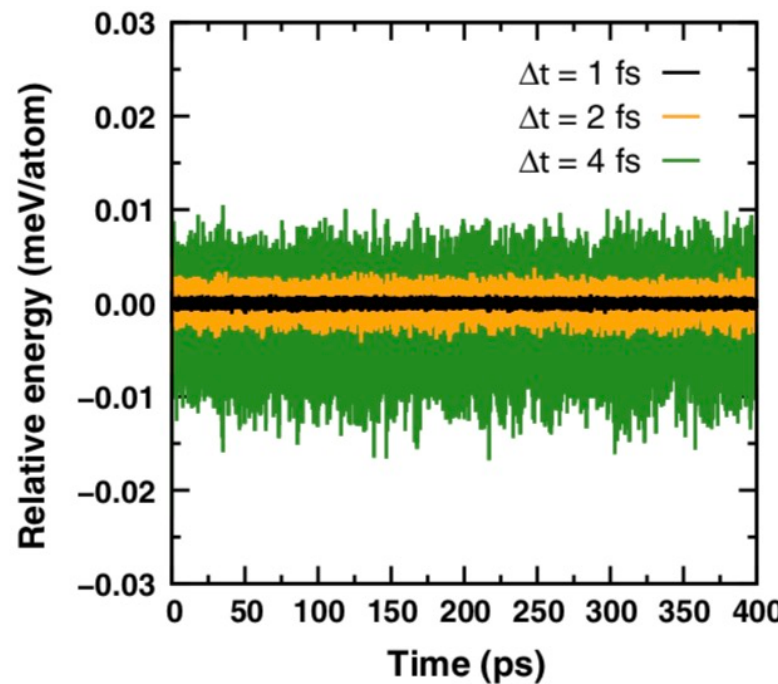


## Error statistics

Smooth change of  
energy with volume

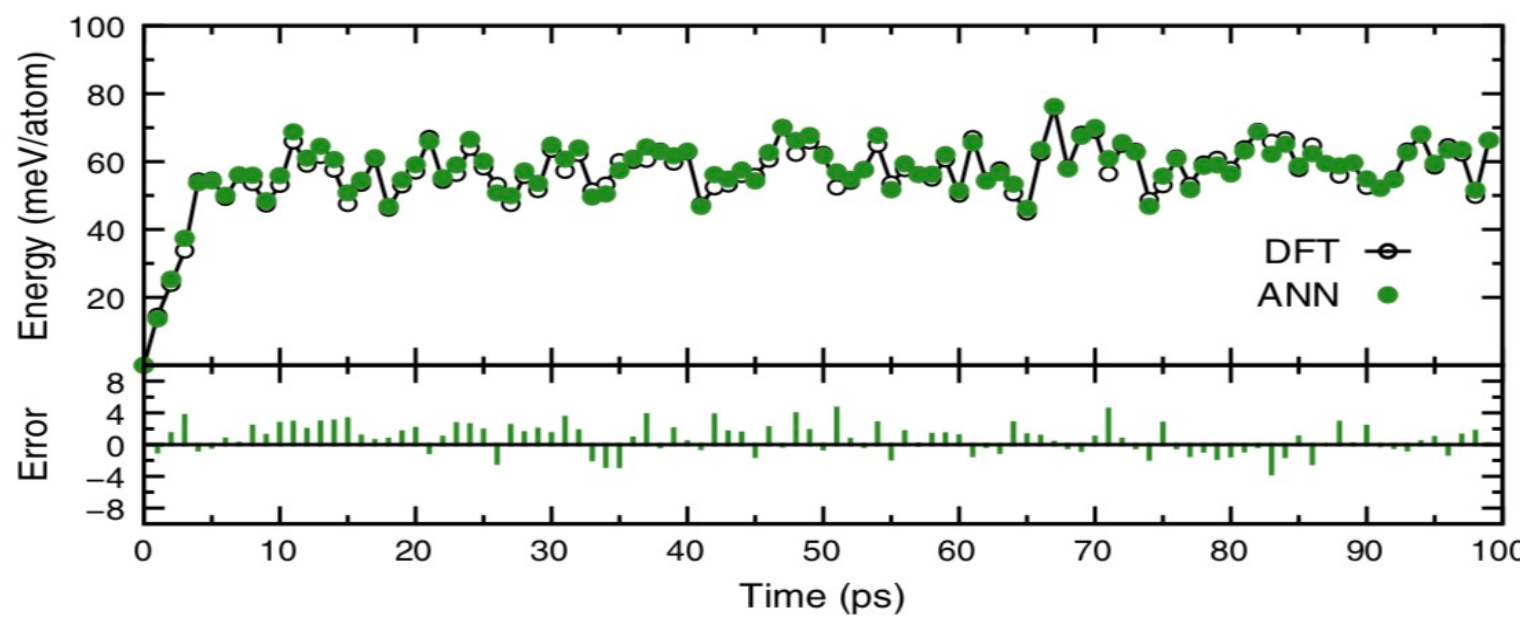


# Reliability of the $\text{TiO}_2$ ANN Potential for MD Runs



NVE runs with  
various timesteps

NVT runs at 500 K  
for different structures





# Machine learning based interatomic potential for amorphous carbon

USC

School of Engineering

University of Southern California



## Basic Ideas & Background

- Interatomic Potential: Mathematical functions for calculating the potential energy of a system of atoms with given positions in space
- Amorphous Carbon(a-C): free, reactive carbon that does not have any crystalline structure
- Tetrahedral Amorphous Carbon (ta-C): a new semiconductor which is able to accept dopants and shows photoconductivity
- GAP: Gaussian approximation potential



## Basic Ideas & Background

- Fast potentials make large-scale molecular-dynamics (MD) simulations possible
- Efficient enough to perform thin-film deposition simulations
- Directly mirroring the atomic-scale processes in experiments

## Shortcomings:

- prominent an underestimated concentration of  $sp^3$ -bonded atoms in *ta-C* and poor description of surfaces.
- density-functional theory(DFT)-based methods are restricted to quite small system sizes and they are limited in practice to a few hundred atoms.



## Key Ideas of Machine Learning (ML)

- map a set of atomic environments directly onto numerical values for energies and forces
- these quantities are “trained” from a large and accurate quantum-mechanical reference database
- interpolated using the ML algorithm

Gaussian approximation potential (GAP):

- Determine the maximum accuracy that any finite-range potential can achieve in a carbon structures.
- Construct a GAP model that can indeed reach the target accuracy, by using a hierarchical set of two-, three-, and many-body structural descriptors.
- Show predictions for energies and structures of ta-C surfaces, which play a key role in wear and fracture mechanisms



## Gaussian approximation potential (GAP)

Energy Function  $\varepsilon$ : energy function is expanded in a basis set adapted to the input database. Generated using a kernel function, or similarity measure of neighbor environments.

Extrapolation: a poor fit in regions of configuration space far away from any data points.

Starting point for the total energy

$$E = (\delta^{(2b)})^2 \sum_{i \in \text{pairs}} \varepsilon^{(2b)}(\mathbf{q}_i^{(2b)}) + (\delta^{(3b)})^2 \sum_{j \in \text{triplets}} \varepsilon^{(3b)}(\mathbf{q}_j^{(3b)}) \\ + (\delta^{(MB)})^2 \sum_{a \in \text{atoms}} \varepsilon^{(MB)}(\mathbf{q}_a^{(MB)}), \quad (1)$$



Local energy corresponding to each descriptor  $d \in \{2b, 3b, MB\}$

$$\varepsilon^{(d)}(\mathbf{q}^{(d)}) = \sum_{t=1}^{N_t^{(d)}} \alpha_t^{(d)} K^{(d)}(\mathbf{q}^{(d)}, \mathbf{q}_t^{(d)}),$$

$$K^{(d)}(\mathbf{q}_i^{(d)}, \mathbf{q}_t^{(d)}) = \exp \left[ -\frac{1}{2} \sum_{\xi} \frac{(q_{\xi,i}^{(d)} - q_{\xi,t}^{(d)})^2}{\theta_{\xi}^2} \right],$$

$\xi$  is an index running over the components of the descriptor vector  $\mathbf{q}(d)$

$$q^{(2b)} = |\mathbf{r}_2 - \mathbf{r}_1| \equiv r_{12};$$

the case of pairs

$$\mathbf{q}^{(3b)} = \begin{pmatrix} r_{12} + r_{13} \\ (r_{12} - r_{13})^2 \\ r_{23} \end{pmatrix}.$$

the case of triplets



# Smooth overlap of atomic positions (SOAP ) descriptor

$$\rho_a(\mathbf{r}) = \sum_b \exp\left[-\frac{(\mathbf{r} - \mathbf{r}_{ab})^2}{2\sigma_{\text{at}}^2}\right] \times f_{\text{cut}}(r_{ab}),$$

$$\rho_a(\mathbf{r}) = \sum_{nlm} c_{nlm}^{(a)} g_n(r) Y_{lm}(\hat{\mathbf{r}}),$$

$$p_{nn'l}^{(a)} = \sqrt{\frac{8\pi^2}{2l+1}} \sum_m (c_{nlm}^{(a)})^* c_{n'lm}^{(a)},$$

the sum is over  
neighboring atoms

$g_n$ : orthogonal radial basis  
functions  
 $Y_{lm}$  : spherical  
harmonics

spherical power spectrum



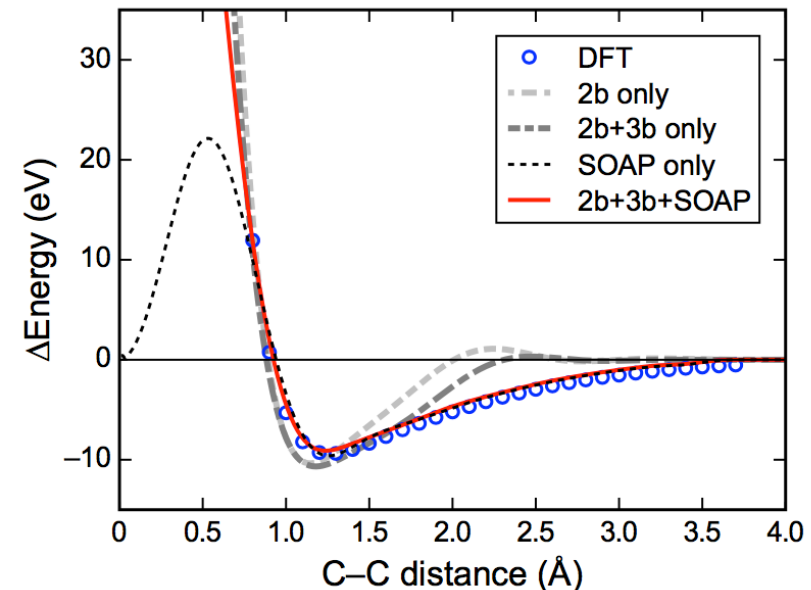
## The kernel function for the SOAP term

$$k(\mathbf{q}_a^{(\text{MB})}, \mathbf{q}_t^{(\text{MB})}) = \sum_{nn'l} p_{nn'l}^{(a)} p_{nn'l}^{(t)} = \mathbf{q}_a^{(\text{MB})} \cdot \mathbf{q}_t^{(\text{MB})}$$

raise it to a small integer power for a sharper distinction between different environments

$$K^{(\text{MB})}(\mathbf{q}_a^{(\text{MB})}, \mathbf{q}_t^{(\text{MB})}) = |\mathbf{q}_a^{(\text{MB})} \cdot \mathbf{q}_t^{(\text{MB})}|^\zeta.$$

$$\begin{aligned} E &= (\delta^{(2\text{b})})^2 \sum_i \sum_t \alpha_t^{(2\text{b})} K^{(2\text{b})}(\mathbf{q}_i^{(2\text{b})}, \mathbf{q}_t^{(2\text{b})}) \\ &+ (\delta^{(3\text{b})})^2 \sum_j \sum_t \alpha_t^{(3\text{b})} K^{(3\text{b})}(\mathbf{q}_j^{(3\text{b})}, \mathbf{q}_t^{(3\text{b})}) \\ &+ (\delta^{(\text{MB})})^2 \sum_a \sum_t \alpha_t^{(\text{MB})} K^{(\text{MB})}(\mathbf{q}_a^{(\text{MB})}, \mathbf{q}_t^{(\text{MB})}), \end{aligned}$$



The expression for the total energy in GAP

All fitting coefficients  $\alpha$  enter linearly



# COMPUTATIONAL METHODS

- General protocol for melt-quench simulations : Structural data were obtained from melt-quench MD, following protocols that are well established for a-C
- DFT-based (“*ab initio*”) molecular dynamics :Structures for initial training, as well as benchmarks for a-C properties, were generated using DFT-based ab initio MD, using the QUICKSTEP scheme and a stochastic Langevin thermostat as implemented in CP2K
- Construction of the training database :contains structural snapshots from ab initio MD and also, as it is iteratively extended, from GAP- driven simulations.

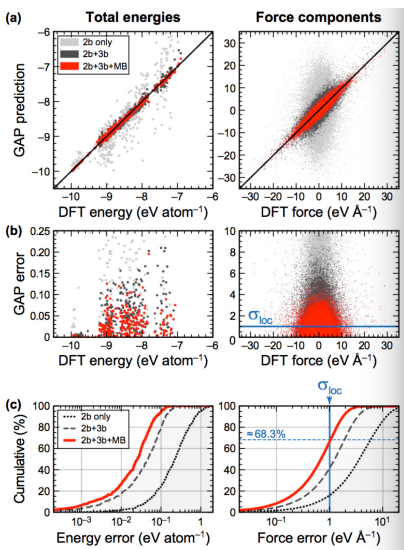
TABLE I. Key parameters for the GAP model created in this work  
(see Sec. II for definitions).

	Two-body	Three-body	SOAP
$\delta$ (eV)	5.0 <sup>a</sup>	0.3 <sup>a</sup>	0.1
$r_{\text{cut}}$ (Å)	3.7	3.0	3.7
$r_{\Delta}$ (Å)			0.5
$\sigma_{\text{at}}$ (Å)			0.5
$n_{\text{max}}, l_{\text{max}}$			8
$\zeta$			4
Sparsification	Uniform	Uniform	CUR
$N_t$ ( <i>a</i> -C bulk)		125	2500
$N_t$ ( <i>a</i> -C surfaces)		50	1000
$N_t$ (crystalline)		25	500
$N_t$ (dimer)			30
$N_t$ (total)	15	200	4030

<sup>a</sup>For the 2b and 3b descriptors, when specifying training input, the  $\delta$  given here is divided by the expected number of pairs or triplets an atom is involved in.



# Results and Discussion



	Energy (eV)	Force components (eV Å <sup>-1</sup> )		
		rms (GAP)	rms (GAP)	P <sub>95</sub> (DFT)
Liquid (9000 K)	0.041	1.27	6.52	0.19
Liquid (5000 K)	0.031	1.12	5.68	0.20
Quench	0.023	1.07	5.06	0.21
Amorphous	0.018	0.94	2.23	0.42
Crystalline	0.002	0.10	1.32	0.08

